Electronic excitation of H_2 by positron impact

F. Arretche and M. A. P. Lima
Instituto de Física "Gleb Wataghin," Universidade Estadual de Campinas, 13083-970, Campinas, São Paulo, Brazil
(Received 20 June 2006; published 12 October 2006)

Recent experiments on electronic excitation of molecules by positron impact have shown much larger cross sections than in the electron scattering case. The challenge of understanding the origin of this enhancement, especially just above electronic excitation thresholds, motivates the search of theoretical explanations of the phenomenon as well as new experimental efforts to confirm the data. In an earlier theoretical effort, an application of the Schwinger multichannel method at two-state level of approximation for the $X\ ^1\Sigma_g^+ \rightarrow B\ ^1\Sigma_u^+$ electronic excitation of the H_2 molecule, gave cross sections with smaller magnitude but reasonable qualitative agreement with the experimental data. The purpose of this work was to study the numerical stability of the previous calculation and to investigate the influence of open channels (energetically accessible electronic states—multichannel effects) and closed channels (energetically inaccessible electronic states—polarization effects) on this transition. Our results show minor multichannel effects and a significative enhancement of the $X\ ^1\Sigma_g^+ \rightarrow B\ ^1\Sigma_u^+$ cross section at the threshold due to polarization effects if compared to the usual static results.

DOI: 10.1103/PhysRevA.74.042713 PACS number(s): 34.85.+x, 34.50.Fa, 34.50.Gb

I. INTRODUCTION

What can we learn from electronic excitation by positron impact? Material science researchers would like to have a better notion about electronic excitation by positron impact in order to improve their models to identify vacancies and defects in crystalline arrays [1]. For astrophysicists, the knowledge of ionization and electronic excitation cross sections (integral and differential) mainly for H, He, and H_2 would be very welcome in order to produce new information about the positron dynamics in the interstellar medium [2]. Finally, the atomic and molecular physics community is actually working to understand the dynamics of positron annihilation in atomic and molecular environments, i.e., direct annihilation and positronium formation processes [3], and the study of other inelastic channels would complement the effort to model the annihilation mechanisms.

From technical point of view, ionization and electronic excitation are considered as the main mechanisms for cooling positrons, after they are generated from radioative decay with keV's of kinetic energy [4]. The comprehension of these inelastic processes may be very useful in the near future to create alternative techniques to produce low energy positron beams. Unfortunately, we can find only few scientific publications (about theories and experiments) on electronic excitation of atoms and molecules by positron impact. Among them, we point out a few studies for noble gases, He [5–9], Ne [6,7,10], Ar [6,7,11,12], and Kr [11], and for simple diatomic molecules as H_2 [12–16], N_2 [12,17,18], and CO [19,20].

Electronic excitation cross sections of H_2 molecules by positron impact were obtained by Mukherjee and Coworkers [13–15] through close-coupling treatment of the problem. Later on, the Schwinger multichannel method (SMC), which was originally designed to describe electron-molecule collisions [21,22], was adapted by Germano and Lima [23] to describe positron-molecule scattering processes. In 1994, Lino *et al.* [16] made an inelastic application of the SMC for positrons to calculate the $X\ ^1\Sigma_g^+ \rightarrow B\ ^1\Sigma_u^+$ electronic excitation cross section of H_2 in a two-state level of approximation. More recently, in 2001, Sullivan *et al.* [12] produced experimental data for this electronic transition induced by positron impact. Comparison with the available theoretical calculations showed that the SMC results were in reasonable agreement with the measured cross sections.

Motivated by these results for H_2, the SMC method was applied to compute electronic excitation by positron impact of N_2 [17,18]. From these applications, a serious difficulty with the trial scattering basis set was identified: numerical instability related to the choice of the variational basis set was producing spurious resonances in the electronic excitation cross section. To overcome the problem, a systematic set of procedures to verify the quality of the basis set, from now on referred as "basis set Born approximation" (BSBA) technique was developed. Because of this unexpected point, the old results for H_2 became suspicious. Here, we repeat the prior calculation and extend the investigation considering the coupling of two ($X\ ^1\Sigma_g^+$ and $B\ ^1\Sigma_u^+$), three ($X\ ^1\Sigma_g^+$, $B\ ^1\Sigma_u^+$, and $E,F\ ^1\Sigma_g^+$) and five ($X^1\Sigma_g^+$, $B\ ^1\Sigma_u^+$, $E,F\ ^1\Sigma_g^+$ and the doubly degenerate $C\ ^1\Pi_u$) states, chosen through their increasing order of threshold energies. The idea was to study how the integral excitation cross sections caused by positrons are affected by the number of available electronic states considered in the theoretical modeling of the scattering process. The calculations for dipole allowed transitions, i.e., $X\ ^1\Sigma_g^+ \rightarrow B\ ^1\Sigma_u^+$ and $X\ ^1\Sigma_g^+ \rightarrow C\ ^1\Pi_u$, showed minor multichannel effects, and this is an unexpected behavior if compared to the electron impact case [24].

It is a fact that when a positron produces the electronic excitation, it transfers energy to the electronic degrees of freedom of the target. If the incident positron has an energy nearly above the electronic excitation threshold, it leaves the target with a very small kinetic energy. From low-energy investigations, it is expected that a slow positron can distort considerably the electronic cloud. To study this effect on the electronic excitation process, we considered target polarization in the energy range immediately above the threshold for $X \rightarrow B$ transition (from now, to simplify the notation, we will

refer to the electronic transitions by the capital letters associated to the spectroscopic notation for the initial and final electronic states considered) but still under the $X \rightarrow E$ threshold. The $X \rightarrow B$ integral cross section with polarization showed considerable enhancement when compared to the pure static calculation.

This paper is organized as follows: in Sec. II we describe the BSBA strategy along with few details of the SMC method for positron scattering, included here to clarify the present application. In Sec. III we show our results for the electronic excitation of H_2 by positron impact. Finally, we present our conclusions in Sec. IV.

II. METHOD

A. Simple considerations on the positron SMC method

We start this section giving a brief summary of the general scheme used in the SMC method to compute the electronic excitation cross sections of molecules by positron impact. The starting point is a given set of Cartesian Gaussian functions $\{G_k\}$ which can be taken from literature, see, for example Refs. [25,26]. From this set of "atomic orbitals," a set of molecular orbitals,

$$\varphi_\mu = \sum_k c_{\mu k} G_k \tag{1}$$

and a ground state wave function

$$\Phi_0(1,2,\ldots,N) = A_N[\varphi_1(1)\bar{\varphi}_1(2)\ldots\varphi_{N/2}(N-1)\bar{\varphi}_{N/2}(N)] \tag{2}$$

are obtained through a restricted Hartree-Fock (RHF) calculation. As shown in the Φ_0 definition, the SMC computer program is presently prepared to deal only with closed shell molecular targets (singlet ground states). By positron impact, only other singlet states can be obtained from a closed shell ground-state target.

From a flexible set of single body wave functions we can construct the molecular electronic excited states $\{\Phi_i, i=1,2,\ldots\}$ and construct a trial basis of the SMC method for the scattering calculation. For the positron wave function we use occupied and virtual orbitals $\{\varphi_k\}$ that come from the Hartree-Fock calculation. These orbitals, combined with the many-body molecular wave functions $\{\Phi_i\}$, allow the construction of the trial scattering basis functions $\{\chi_{ij}\}$,

$$\chi_{ij} = \Phi_i(1,2,\ldots,N) \otimes \varphi_j(p), \tag{3}$$

which are just direct products between the molecular wave functions ($\{\Phi_i\}$) and positron scattering orbitals ($\{\varphi_j\}$). The occupied orbitals of the Hartree-Fock target are also included in the basis set expansion because the positron is not identical to the target electrons and no orthogonality condition must be enforced between electron and positron orbitals. We then assume that this set is complete, i.e.,

$$\sum_{ij} |\chi_{ij}\rangle\langle\chi_{ij}| \approx 1, \tag{4}$$

and expand the scattering wave function in this basis,

$$\Psi_{\vec{k}}^{(\pm)} = \sum_{ij} a_{ij}^{(\pm)}(k)\chi_{ij}. \tag{5}$$

The best set of expansion coefficients ($a_{ij}^{(\pm)}$) is obtained by maximizing the bilinear form of the scattering amplitude with respect to them [23]. This gives the working expression for the scattering amplitude used in the SMC method, i.e.,

$$f_{\vec{k}_i \rightarrow \vec{k}_f}^{SMC} = -\frac{1}{2\pi}\sum_{mn}\langle S_{\vec{k}_f}|V|\chi_m\rangle(d^{-1})_{mn}\langle\chi_n|V|S_{\vec{k}_i}\rangle \tag{6}$$

with

$$d_{mn} = \langle\chi_m|PVP + Q\hat{H}Q - VG_P^{(+)}V|\chi_n\rangle. \tag{7}$$

Briefly, $S_{\vec{k}}$ is a solution of the unperturbed Hamiltonian (molecular Hamiltonian plus the kinetic energy operator for the incident positron), P and Q are projectors onto energetically open and closed states of the target, V is the scattering potential, $\hat{H}$ is the total energy minus the scattering Hamiltonian, $G_P^{(+)}$ is the projected Green's function, and $\{\chi_m\}$ are the $(N+1)$-particle trial scattering functions formulated as showed above.

Once the scattering amplitude is obtained, we calculate the associated integral cross section for the considered collision channel through the following standard expression:

$$\sigma^{i\rightarrow f} = \frac{1}{4\pi}\frac{k_f}{k_i}\int d\Omega_{\vec{k}_i}\int d\Omega_{\vec{k}_f}|f_{\vec{k}_i\rightarrow\vec{k}_f}^{SMC}|^2. \tag{8}$$

B. Basis set Born approximation technique

To define a good Cartesian Gaussian basis set to produce a scattering calculation is not an easy task and the experience gained in *ab initio* calculations for electron-molecule collisions can be useful. As pointed out by Carsky [27], up to date, there are no clear rules or procedures to construct trial scattering basis sets for *ab initio* scattering calculations. The ideia is to work with an initial set of functions $\{G_k\}$ large enough such that the completeness of the basis set comes from "saturation":

$$\sum_k |G_k\rangle\langle G_k| \approx 1. \tag{9}$$

The usual practice is to start with a flexible set of Cartesian Gaussian functions, ordinarily used in molecular orbital theory, and then add to this initial set diffuse valence and diffuse polarization functions in order to better describe the scattering wave function.

The SMC method is a variational approach for the scattering amplitude. For the energy range considered in this work (13.5 to 30.0 eV), the elastic integral cross section is of order a_0^2. Usually, the electronic excitation cross sections are at least one order of magnitude smaller than the elastic one. The experience with N_2 [17,18] has shown that electronic excitation cross sections demand trial scattering basis sets with a higher degree of refinement than for pure elastic calculations.

Consider the prescription for the scattering amplitude given in the first Born approximation (FBA),

$$f^{FBA}_{\vec{k}_i\to\vec{k}_f} = -\frac{1}{2\pi}\langle S_{\vec{k}_f}|V|S_{\vec{k}_i}\rangle = -\frac{1}{2\pi}\int d^3r_p e^{i(\vec{k}_i-\vec{k}_f)\cdot\vec{r}_p}\langle\Phi_f|V|\Phi_i\rangle, \tag{10}$$

where $S_{\vec{k}_\ell}$ are solutions of Schödinger equation for the free Hamiltonian,

$$S_{\vec{k}_\ell} = \Phi_\ell(1,2,\ldots,N)\otimes e^{i\vec{k}_\ell\cdot\vec{r}_p}, \tag{11}$$

and V is the Coulombic interaction between the incident positron and the molecular target.

If we use the operator V in its fractional form $(VV^{-1}V)$ in Eq. (10) with the introduction of our "complete" trial scattering basis set $\{\chi_{ij}\}$, we obtain

$$f^{BSBA}_{\vec{k}_i\to\vec{k}_f} = -\frac{1}{2\pi}\sum_{mn}\langle S_{\vec{k}_f}|V|\chi_m\rangle[(PVP)^{-1}]_{mn}\langle\chi_n|V|S_{\vec{k}_i}\rangle, \tag{12}$$

which is called basis set Born approximation (BSBA) for the scattering amplitude. We introduced a projection operator P because in this prescription we consider only basis vectors related to energetically open electronic states.

Observe that Eq. (12) for the scattering amplitude is equal to the SMC one [Eq. (6)], provided the correlation $(Q\hat{H}Q)$ and Green's function terms $(VG_P^{(+)}V)$ are dismissed.

Scattering amplitudes obtained from FBA are valid for high-energy static calculations, i.e., in situations where the target wave functions can be considered frozen. Provided good wave functions are employed, the FBA cross section is nearly basis set independent. Besides, as FBA treats the positron as a plane wave, no resonances should be found in the cross section and for any energy the annihilation parameter Z_{eff} calculated with the FBA scattering wave function must be equal to Z [28].

Since BSBA is just an adaptation of the FBA, the cross section obtained through BSBA gives a direct and unequivocal measure of the quality of the expansion $\Sigma_m|\chi_m\rangle\langle\chi_m| \approx 1$. If the trial scattering basis set is "good enough," it is expected that $\sigma^{BSBA} \approx \sigma^{FBA}$ and also $Z^{BSBA}_{eff} \approx Z$, where Z^{BSBA}_{eff} is just the annihilation parameter calculated from BSBA scattering wave function.

The BSBA cross sections computed in N_2 applications showed resonances [17,18]. These are obviously nonphysical. The cause of these spurious structures are due to the presence of basis vectors weakly coupled to the scattering potential, i.e., very small matrix elements of the form $\langle\chi_m|PVP|\chi_m\rangle$. These very small numbers could give rise to very large numbers in the matrix inversion [see Eq. (12)] producing the nonphysical resonances. To overcome this difficulty, Chaudhuri *et al.* [17,18] developed a set of procedures to repair the original trial scattering basis set. These are the following:

(1) Diagonalize the matrix $\langle\chi_m|PVP|\chi_n\rangle$.

(2) From this diagonalization we obtain a set of eigenvectors $\{\tilde{\chi}_m\}$ and eigenvalues $\{\lambda_m\}$,

$$(PVP)|\tilde{\chi}_m\rangle = \lambda_m|\tilde{\chi}_m\rangle \tag{13}$$

and a transformation matrix R, that relates the old set of vectors $\{\chi_m\}$ with the new one $\{\tilde{\chi}_m\}$,

$$|\tilde{\chi}_m\rangle = \sum_n R_{mn}|\chi_n\rangle. \tag{14}$$

(3) Rotate the original vectors to work with the set of eigenvectors of the scattering potential, $\{\tilde{\chi}_m\}$.

(4) Disregard the basis vectors $|\tilde{\chi}_m\rangle$ associated with eigenvalues smaller, in absolute value, than a given threshold λ_{max}.

(5) Verify that $Z^{BSBA}_{eff} \approx Z$ within an arbitrary range of tolerance and that $\sigma^{BSBA} \approx \sigma^{FBA}$.

(6) If $Z^{BSBA}_{eff} \approx Z$ and $\sigma^{BSBA} \approx \sigma^{FBA}$ are simultaneously satisfied, the basis set is considered ready to be employed in the overall scattering calculation. If this is not the case, increase λ_{max} and go back to step (4).

C. Born-closure scheme to treat high-energy scattering

When dealing with dipole allowed transitions, such as $X\,^1\Sigma_g^+ \to B\,^1\Sigma_u^+$ and $X\,^1\Sigma_g^+ \to C\,^1\Pi_u$, the long-range character of the dipolar coupling requires a large number of partial waves [29]. The SMC codes are actually performing calculations with Cartesian Gaussian functions of s, p and d types. Because of it, the "higher partial waves" are not well described.

To repair this deficiency, a Born-closure (BC) scheme was applied. It consists of combining the SMC scattering amplitude with the FBA one. From the FBA amplitude we can obtain

$$F^{FBA}_{\ell,m}(k_f,\vec{k}_i) = \int Y^*_{lm}(\hat{k}_f) f^{FBA}_{\vec{k}_i\to\vec{k}_f} d\Omega_{\hat{k}_f}. \tag{15}$$

The SMC scattering amplitude can be further decomposed in partial waves:

$$f^{SMC}_{\vec{k}_i\to\vec{k}_f} = \langle\vec{k}_f|f^{SMC}|\vec{k}_i\rangle = \sum_{\ell m\ell' m'}^{\ell'_{max}} Y^m_\ell(\hat{k}_f)\langle\ell m|f^{SMC}|\ell' m'\rangle Y^{m'\star}_{\ell'}(\hat{k}_i). \tag{16}$$

The contribution from high-angular-momentum partial waves can then be accounted by means of a BC procedure. In this case, for angular momenta up to a given value ℓ'_{max}, the contributions to the cross section were obtained from the Schwinger variational calculation, while the first Born approximation (FBA) was used to include contributions above ℓ'_{max} up to ℓ_{max}, that is,

$$\begin{aligned} F^{BC}_{\ell,m}(k_f,\vec{k}_i) &= \langle\ell m|f^{BC}|\vec{k}_i\rangle = F^{FBA}_{\ell,m}(k_f,\vec{k}_i) \\ &+ \eta\sum_{\ell',m'}^{\ell'_{max}}[\langle\ell m|f^{SMC}|\ell' m'\rangle \\ &- \langle\ell m|f^{FBA}|\ell' m'\rangle]Y^{m'\star}_{\ell'}(\hat{k}_i), \end{aligned} \tag{17}$$

where $\eta=0$ for $\ell'_{max} < \ell \le \ell_{max}$ and $\eta=1$ for $0 \le \ell \le \ell'_{max}$. In the present calculations we have used $\ell'_{max}=2$ and $\ell_{max}=9$.

TABLE I. Vertical excitation energies for the three lower singlet states of H_2 molecule in electron volts (eV).

State	IVO	R matrix [35]	Exact	Experiment [38]
$B\ ^1\Sigma_u^+$	12.74	13.15	12.75 [36]	11.19
$E,F\ ^1\Sigma_g^+$	13.01	13.25	13.14 [36]	12.35
$C\ ^1\Pi_u$	13.12	13.11	13.23 [37]	12.30

III. RESULTS

A. Computational details

In order to verify the existence of numerical instabilities in the former application of the SMC method to electronic excitation we have used the BSBA strategy to perform calculations with the two Gaussian basis sets of Ref. [16] considering also the same set of impact energies: 13.5, 15.0, 17.5, 20.0, 22.5, 25.0, 27.5, and 30.0 eV. The first set, which was originally applied in elastic electron-H_2 scattering [30], was incremented with three d-type uncontracted functions with exponents 4.5, 0.5, and 0.25 in each hydrogen atom in order to improve the higher partial waves description. From now on this incremented basis will be called "basis 1." The second set of Ref. [16] was originally employed in electron-H_2 scattering for the electronic excitation of the first triplets states of the H_2 molecule [31]. Later on, it was also used for the excitation of the $B\ ^1\Sigma_u^+$ state of H_2 [29]. More recently, few extra Gaussian functions were added to this basis to perform a study about the coupling of singlets and triplets in electron-H_2 scattering [32,33]. Here we have used this more incremented basis and in what follows we will call it "basis 2."

The wave functions for the excited electronic states were all generated with the improved virtual orbital (IVO) method [34]. Table I shows vertical excitation energies compared to theoretical [35–37] and experimental [38] data. Basis 1 was used only in the two-state calculations and has practically the same vertical excitation energy as basis 2.

B. Results for $X \rightarrow B$ transition: Application of BSBA technique

In Fig. 1 we show the FBA integral cross section for the $X \rightarrow B$ electronic transition compared with the BSBA for the two basis. Note that σ^{FBA} is equal for both basis. On the other hand direct inspection of Fig. 1 shows that $\sigma^{BSBA} \neq \sigma^{FBA}$ for the two basis sets.

Figure 2 shows the Z_{eff} calculated in BSBA (Z_{eff}^{BSBA}) before and after the basis set treatment. Here, we considered as satisfactory, values of Z_{eff}^{BSBA} between 1.8 and 2.2, giving a tolerance of 10% relative to Z. We can easily see that after removing the spurious basis vectors, the values of Z_{eff}^{BSBA} satisfy this criterion and the remaining basis vectors of each set are considered ready for electronic excitation calculations.

Figure 3 displays the σ^{FBA} and σ^{BSBA} with the treated basis sets. The improvement in the σ^{BSBA} calculation is clear. The results with the Born-closure scheme are also shown. It is evident that this scheme is necessary in the "high" energy region ($E \geq 20.0$ eV).

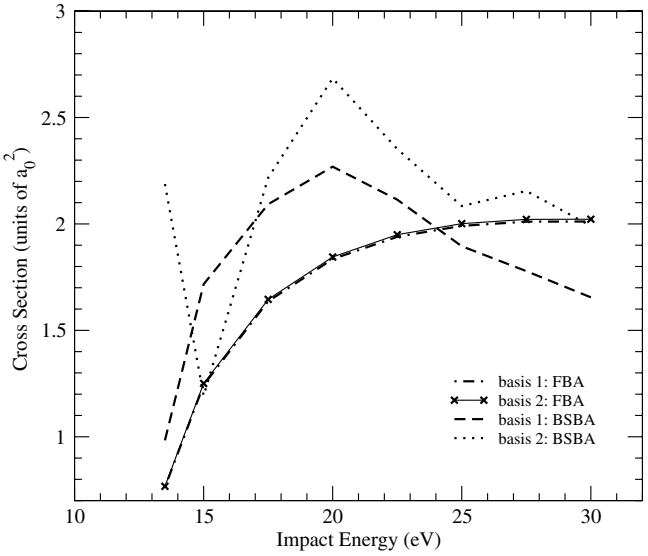

FIG. 1. Electronic excitation cross section for $X\ ^1\Sigma_g^+ \rightarrow B\ ^1\Sigma_u^+$ in units of a_0^2. Dot-dashed line: FBA cross section for basis 1; line with crosses: FBA for basis 2; dashed line: BSBA for basis 1; dotted line: BSBA for basis 2.

After treating the scattering basis set according to the BSBA, we have used this scattering basis set to obtain cross sections with the SMC method. First, in Fig. 4 we present the electronic excitation cross section with the complete original sets of scattering basis vectors. These calculations were produced with two different approaches for the evaluation of the

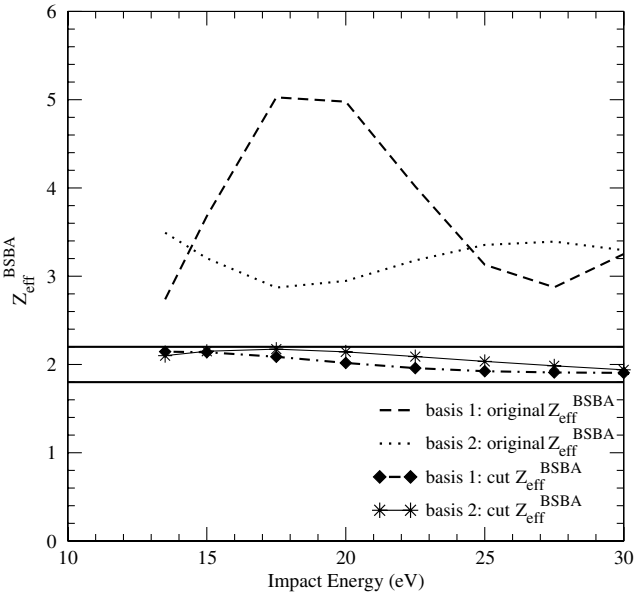

FIG. 2. Z_{eff}^{BSBA} before and after removing the spurious trial scattering basis vectors. Dashed line: original results for Z_{eff}^{BSBA} produced by basis 1; dotted line: the same, but for basis 2; dot-dashed line with diamonds: results obtained for Z_{eff}^{BSBA} after removing the spurious basis vectors for basis 1; line with stars: the same, but for basis 2. The full straight lines above and below $Z_{eff}^{BSBA} = 2$ represents the upper (2.2) and lower (1.8) limits considered as satisfactory for Z_{eff}^{BSBA}.

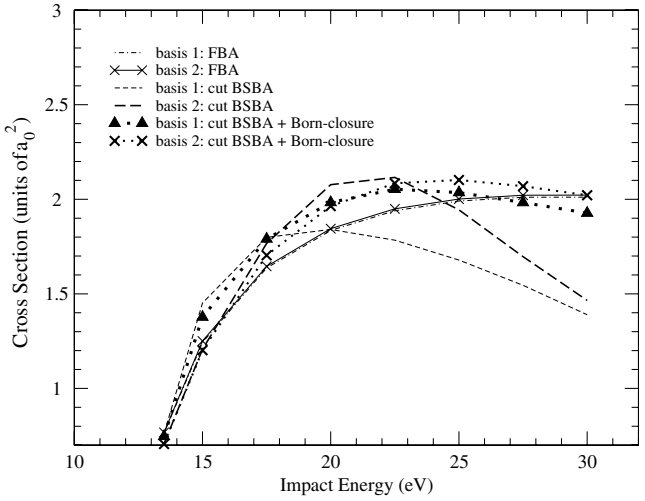

FIG. 3. Electronic excitation cross section for $X\ ^1\Sigma_g^+ \rightarrow B\ ^1\Sigma_u^+$ in units of a_0^2. The thin dot-dashed line: FBA cross section for basis 1; thin line with crosses: FBA for basis 2; thin dashed line: treated (cut) BSBA for basis 1; gross dashed line: the same, but for basis 2; line of points with triangles: Born-closure for treated (cut) BSBA for basis 1; line of points with crosses: the same, but for basis 2.

Green's function matrix elements. The first approach is called k insertion [39] (in this approach, the residue contribution from the VGV term is calculated by numerical quadrature and principal value is obtained by insertion of unit operator, constructed from Cartesian Gaussian functions) and it is based on the original strategy used in SMC to compute the Green's function matrix elements. The central idea lies in the spectral decomposition of a plane wave onto a finite Gaussian basis, which provides analytical expressions. Because the required number of Gaussian functions to obtain convergence increased substantially with the target's size and with the number of considered collision channels, a second method was developed. It is called 3dk-insertion method [40] (in this approach, the residue and the principal value terms of the Green's function are obtained from numerical quadrature). In 3dk insertion, the integration over linear momentum variables arising in $VG_P^{(+)}V$ matrix elements are performed by numerical quadrature. Additional details can be found in Ref. [39].

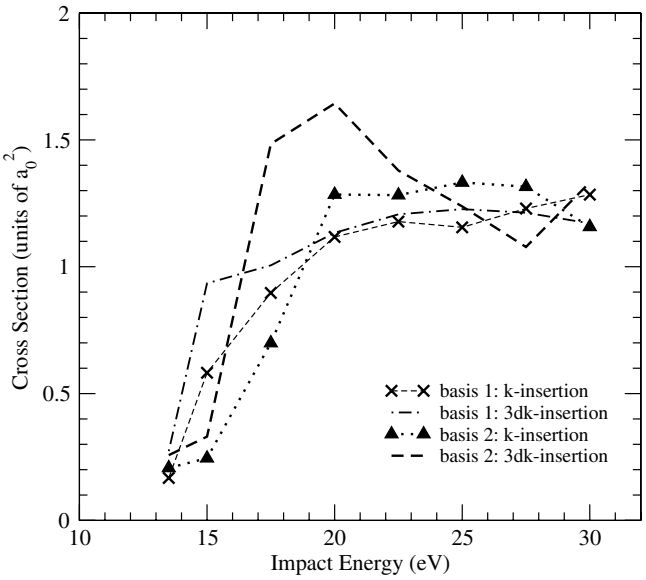

FIG. 4. Electronic excitation cross section for $X\ ^1\Sigma_g^+ \rightarrow B\ ^1\Sigma_u^+$ in units of a_0^2 produced with SMC method. The dashed line with crosses: cross section for original basis 1 with k-insertion method; dot-dashed line: the same but with 3dk method; dotted line with triangles: cross section for original basis 2 with k-insertion method; dashed line: the same, but with 3dk method.

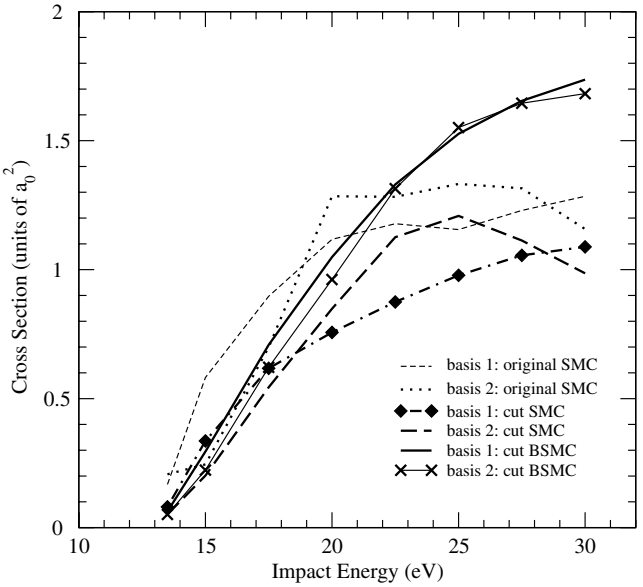

FIG. 5. Electronic excitation cross section for $X\ ^1\Sigma_g^+ \rightarrow B\ ^1\Sigma_u^+$ in units of a_0^2 produced with SMC method using k-insertion method. The thin dashed line: cross section for original basis 1; dotted line: the same, but for basis 2; dot-dashed line with diamonds: treated (cut) SMC results for basis 1; gross dashed line: the same but for basis 2; full line: treated (cut) SMC results with Born-closure scheme (BSMC); full line with crosses: the same, but for basis 2.

It is evident, from Fig. 4, that discrepancies in the cross sections are found in the SMC calculations with the two scattering complete basis sets and with different insertion techniques of the VGV term. An optimistic could say that at least the cross sections have the same order of magnitude and float around a smooth curve. In Fig. 5 we present the results obtained with the treated scattering basis sets and with the k-insertion method. The results with the two basis sets get very similar after the treated SMC calculations receives the Born-closure complement. In Fig. 6 we show the same sort of results for the 3dk-insertion method, used to evaluate the VGV term. Basically the same comments are valid.

In Fig. 7, for basis set 2, we compare the calculated cross sections using the two methods of evaluating the VGV term. Analysis of the figure shows good agreement between the two methods. This is of special relevance for the SMC method, since the 3dk-insertion method demands great computational effort compared to the k-insertion method. Similar results, not shown, were found for basis set 1. These results motivated us to further explore the BSBA method.

Finally, in Fig. 8 we present the results obtained in these calculations compared to the old ones and to the other

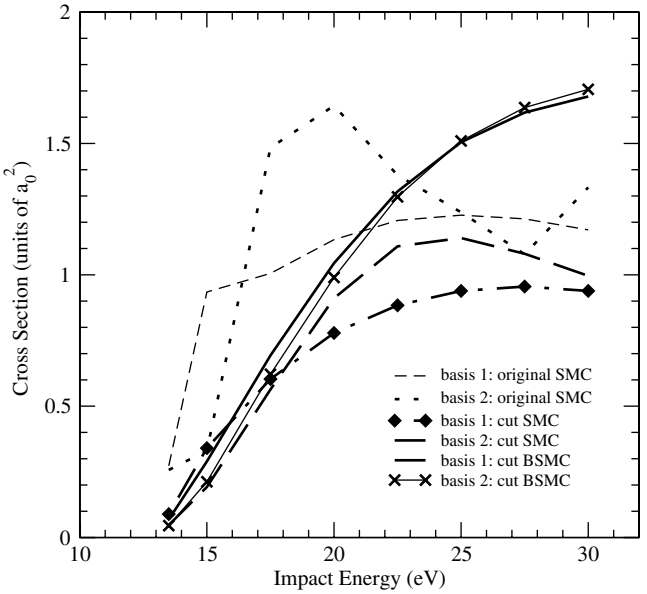

FIG. 6. The same as Fig. 5 but for 3*dk*-insertion method.

available data reported in literature. The great similarity between the prior and the new calculation up to 25.0 eV is evident. Lino *et al.* [16] obtained this electronic excitation cross section by "try and error," i.e., starting with a given basis set (here, we refer to the set of Gaussian functions), they were able to add and adjust Gaussian functions to a second different basis set until convergence was achieved. In this work, the electronic excitation cross section was

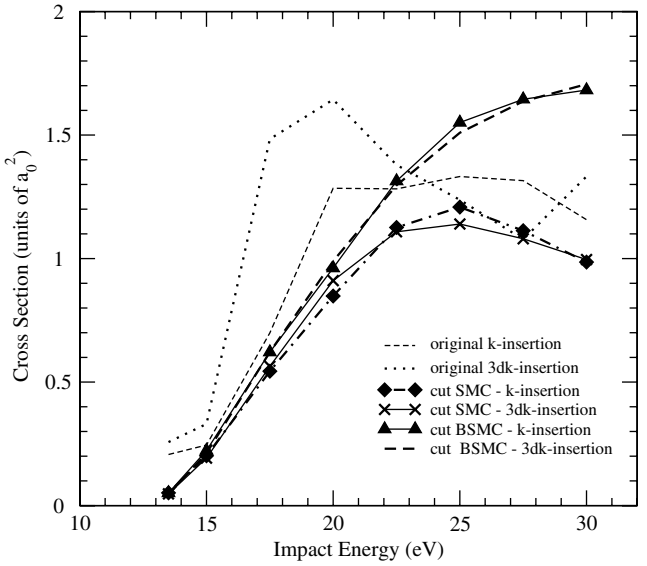

FIG. 7. Electronic excitation cross section for $X\,^1\Sigma_g^+ \rightarrow B\,^1\Sigma_u^+$ in units of a_0^2 produced with SMC method using *k* and 3*dk*-insertion methods for basis 2. The thin dashed line: cross section for k-insertion method with the original trial scattering basis set; dotted line: the same, but for 3*dk* method; dot-dashed line with diamonds: cut SMC results for *k* insertion; full line with diamonds: the same but for 3*dk* insertion; full line with triangles: cut SMC results with Born-closure scheme (BSMC); gross dashed line: the same, but for 3*dk* insertion.

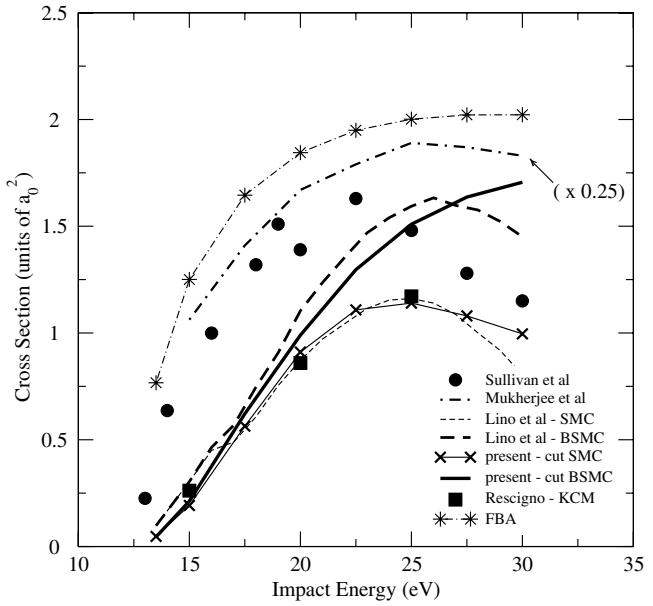

FIG. 8. Final results for integral electronic excitation cross section for $X\,^1\Sigma_g^+ \rightarrow B\,^1\Sigma_u^+$ in units of a_0^2. The black circles: experimental data of Sullivan *et al.* [12]; dot-dashed line: calculation of Mukherjee *et al.* [13] multiplied by 0.25; thin dashed line: prior SMC result presented in Lino *et al.* [16]; gross dashed line: prior SMC result with Born-closure scheme (BSMC); full line with crosses: present cut SMC results for basis 2 with 3*dk*-insertion method; gross full line: present cut SMC results with Born closure scheme; squares: Kohn complex method (KCM) calculation [41]. Dot-dashed line with stars: FBA results.

generated through a systematic treatment of the set of trial scattering basis functions $\{\chi_{ij}\}$ and practically does not depend of the initial set of Gaussians employed in the quantum-chemical description of the molecular target, i.e., as long as it is large enough to produce a proper description of scattering dynamics.

Above 25.0 eV the obtained integral cross section does not decreases as the old one. This is due to the closure scheme employed in the former calculation where only the outgoing scattering partial waves were completed with the first Born waves. Also, this last figure shows results obtained by the Kohn complex method (KCM) [41] for 15, 20, and 25 eV. Since this application of the Kohn method does not use the Born-closure scheme, the comparison should be done directly with pure SMC results. It is found an excellent agreement between the KCM calculated cross sections and the SMC ones. We also show the FBA cross section for this electronic transition and find it with the same order of magnitude as the more sophisticated calculations. This is somehow unexpected and it may be fortuitous. This point demands further investigation.

C. Results for multichannel calculations

To test the stability of the $X \rightarrow B$ cross section, we have performed calculations beyond the two-state level of approximation, presented above. We have carried out calculations in three- and five-state levels of approximations. The

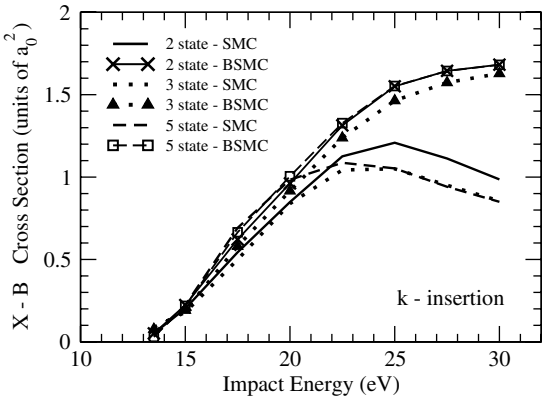

FIG. 9. Multichannel results with k-insertion method for the electronic excitation $X\,^1\Sigma_g^+ \rightarrow B\,^1\Sigma_u^+$ in units of a_0^2. Full line: two-state results generated by SMC; full line with crosses: the same but with the Born-closure (BSMC) scheme; dotted line: three-state results by SMC; dotted line with triangles: the same but with BSMC; dashed line: five-state results by SMC; dashed line with squares: the same but with BSMC.

three state was done considering the ground (X), B and E states. The five-state calculation considered also the C state which is doubly degenerate. These are the next two singlet electronic states in increasing order of energy.

The results for $X \rightarrow B$ cross section are presented in Figs. 9 and 10 considering the two methods for calculation of the Green's function matrix elements. Comparing these figures, we see excellent agreement between the results generated by k and $3dk$-insertion methods. The presence of the E state as an open channel does not disturb the $X \rightarrow B$ cross section, which should not be a surprise. The transition $X \rightarrow E$ is of lower intensity because it happens between even (g) states. But, the five-state calculation produces a nonusual result since, the competition with the C state did not produce any significant change in the $X \rightarrow B$ cross section. It is unexpect because in electron scattering the competition between these collision channels is relevant [24].

In Fig. 11 we show the $X \rightarrow E$ electronic transition. Since this is not of long-range character, it is not necessary to consider the Born-closure procedure. If we are not so rigorous, we can see that the three channel calculation produced

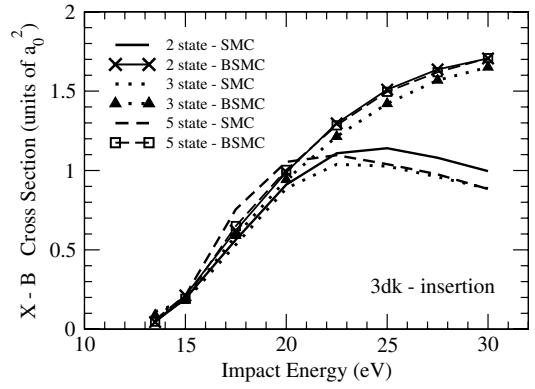

FIG. 10. Exactly the same as in Fig. 9 but using the $3dk$-insertion method.

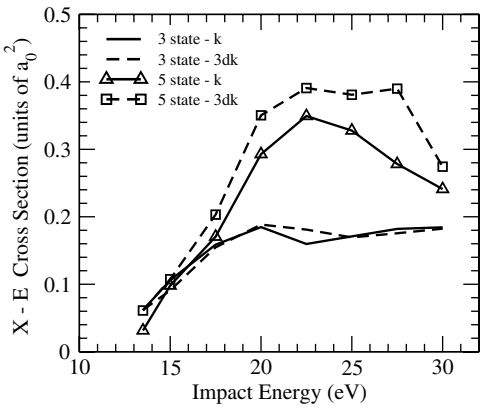

FIG. 11. Multichannel results for the electronic excitation $X\,^1\Sigma_g^+ \rightarrow E, F\,^1\Sigma_g^+$ in units of a_0^2. Full line: three-state results generated with k-insertion method; dashed line: the same but with $3dk$ method; full line with triangles: five-state results generated with k insertion; dashed line with squares: the same but with $3dk$ method.

similar results using the two Green's function methods. Note, however, that the five-state calculation is different from the three-state one for this transition. This may be a natural consequence of multichannel effects. In this calculation, the $X \rightarrow E$ channel has to compete with other four electronic transitions of higher intensity, i.e., the elastic, $X \rightarrow B$ and $X \rightarrow C$. The integral cross section associated with this excitation is, therefore, much more sensible to the multichannel theoretical modeling of the collision process.

The results for the $X \rightarrow C$ transition are shown in Fig. 12. Again, we see reasonable convergence between k- and $3dk$-insertion methods. This figure also indicates a nontrivial result: the cross section associated with the $X \rightarrow C$ transition is similar to the $X \rightarrow B$ one. Figure 13 shows, indeed, that they are very similar. The compared data correspond to the five-state calculation generated by $3dk$-insertion method. These results can motivate experiments (similar to the B state of Ref. [12]) for the $X \rightarrow C$ transition. It is important to point out that this level of similarity for these cross sections can also be noted in a equivalent five-state calculation for electron scattering (see Ref. [24]).

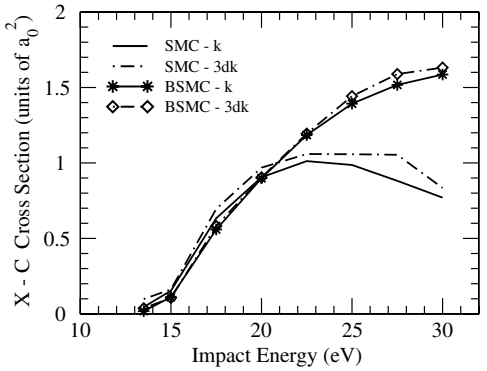

FIG. 12. Results for the electronic excitation $X\,^1\Sigma_g^+ \rightarrow C\,^1\Pi_u$ in units of a_0^2. Full line: five-state result generated with k-insertion method by SMC; dot-dashed line: the same but with $3dk$ insertion; full line with stars: five-state results generated with k-insertion with the Born-closure scheme (BSMC); dot-dashed line with diamonds: the same but with $3dk$ method.

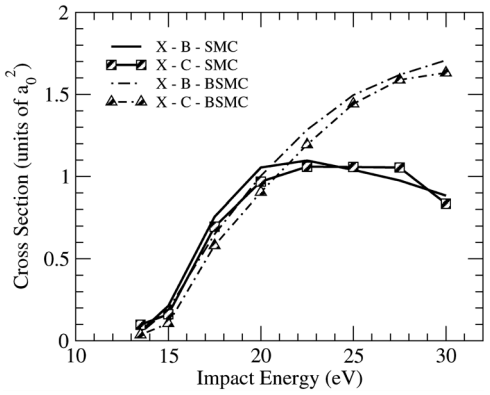

FIG. 13. Comparison for the electronic excitations $X\,^1\Sigma_g^+ \rightarrow B\,^1\Sigma_u^+$ and $X\,^1\Sigma_g^+ \rightarrow C\,^1\Pi_u$ generated in the five-state level of approximation with $3dk$ method in units of a_0^2. Full line: $X \rightarrow B$ cross section by SMC; full line with squares: $X \rightarrow C$ cross section by SMC; dot-dashed line: $X \rightarrow B$ cross section with Born-closure scheme (BSMC); dot-dashed line with triangles: the same but for the $X \rightarrow C$ transition.

D. Polarization effects in $X \rightarrow B$ transition

Positrons with incident energies immediately above the threshold for electronic excitation can leave the target, after the collision, with very low kinetic energies. The electronic excited states often present different values for characteristic molecular quantities such as dipole moments and polarizabilities compared to the ground state. Some electronic excitation transitions can place electrons away from the nuclei, stimulating virtual positronium formation. In this context, a favorable scenario for positron trapping in the target field can be formed.

Specifically, we considered the energy range between 12.74 and 13.01 eV. In this situation the $X \rightarrow$ B transition is energetically allowed while the $X \rightarrow E$ is still a closed channel. Because of the low positron speed after electronic excitation, we considered polarization effects through virtual excitations of the molecular target [23], which compose the closed channel space for the trial scattering basis functions.

We present our results in Fig. 14. We compare the static results with the polarization ones, calculated by the k- and $3dk$-insertion methods. The figure shows a significative enhancement of the electronic excitation cross section with the inclusion of polarization.

In the past, we learned that a good description of polarization can demand the inclusion of extra centers in the Gaussian basis set around the molecule [42]. In this case, we used a cube of size 2 a_0 centered at the geometric center of the molecule with Gaussian functions of s and p types with exponent 0.75 at each corner of the cube.

Looking at Fig. 14, we see that the static results obtained with the inclusion of the cubic arrangement of functions have lower magnitude in comparison to the ones calculated without these functions. They have, however, similar behavior. We also see that the polarization results obtained with the cubic arrangement are converged to the prior ones. Figures 15 and 16 show that at the static level of approximation the extra functions in the cube affect the cross sections just above threshold and that for higher energies ($E \geq 14.0$ eV) the static results are well converged. The inclusion of polarization brings the two results together, which is a very good evidence for the plausibility of the physical effect, and increases substantially the cross sections between the two thresholds. We included in this figure, the measured cross section reported by Sullivan *et al.* [12] for $E=13.0$ eV, which is the only measured energy avaliable for direct com-

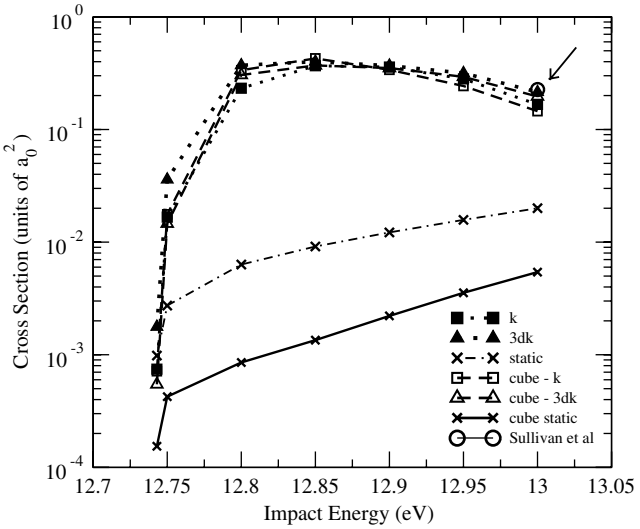

FIG. 14. Integral electronic excitation cross section for $X\,^1\Sigma_g^+ \rightarrow B\,^1\Sigma_u^+$ in units of a_0^2 at the threshold energy region considering polarization effects. Dotted line with full squares: k-insertion result with polarization; dotted line with full triangles: $3dk$-insertion result with polarization; dotted-dashed line with crosses: static result; dashed line with open squares: k insertion with cubic arrangement and polarization; dashed line with open triangles: $3dk$ insertion with cubic arrangement and polarization; full line with crosses: static result with cubic arrangement; round point indicated by the arrow: experimental result of Sullivan *et al.* [12] for 13.0 eV.

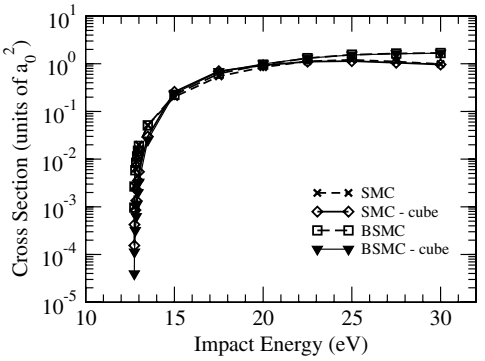

FIG. 15. Integral electronic excitation cross section for $X\,^1\Sigma_g^+ \rightarrow B\,^1\Sigma_u^+$ in units of a_0^2 for the whole energy range in the static approximation with and without the cubic arrangement of functions. All results are from k-insertion method. Dashed line with crosses: SMC cross section; full line with diamonds: SMC result with the cubic arrangement of functions; dashed line with squares: SMC with Born-closure (BSMC); full line with triangles down: SMC with Born-closure (BSMC) with the cubic arrangement of functions.

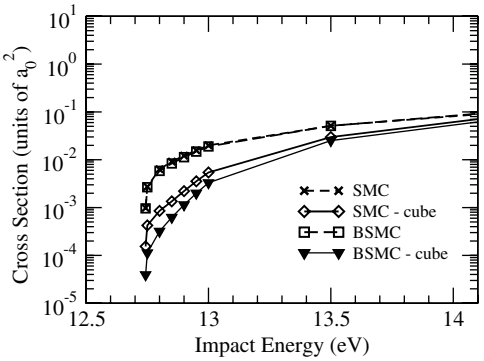

FIG. 16. The same as in Fig. 15 but for energies closer to the $X \rightarrow B$ excitation threshold.

parison in this energy range. The agreement between our theoretical results and the experimental point is very good.

The present results indicate that correlation-polarization between the incident positron and the electronic cloud can be extremely relevant to calculate electronic excitation cross sections for energies close to excitation thresholds.

IV. CONCLUSIONS

In this work we applied the BSBA technique to positron-H_2 electronic excitation. The prior calculation [16] for the $X \rightarrow B$ transition was practically verified until 25.0 eV. Above this energy, the new cross section does not fall as the old one and the experimental data [12].

We verified unquestionable convergence of electronic excitation cross sections relative to the methods for calculation of Green's function matrix elements, i.e., by *k*-insertion and 3*dk*-insertion methods for pure static and static plus polarization calculations. It reinforces the quality of the present *ab initio* results and has practical consequences since the 3*dk*-insertion method for the *VGV* term is more expensive from computational point of view.

The calculations were carried out with different levels of approximation, i.e., two, three, and five open channels, and these showed excellent convergence for the $X \rightarrow B$ transition indicating minor multichannel effects for positron electronic excitation. This point deserves further investigation. Also, the fact that the $X \rightarrow B$ and $X \rightarrow C$ cross sections are practically equal in the energy range studied constitutes a theoretical result with possible experimental investigation considering the actual "state of art" of the area. The calculations showed that the $X \rightarrow E$ cross section demands a refined degree of description because this transition is of lower intensity compared to the other ones and is more sensitive to the level of multichannel coupling used in the description of the collision process.

We observed that the inclusion of polarization effects in the energy range nearly above the electronic excitation threshold can produce significative enhancement of the electronic excitation cross sections, as it was shown for the $X \rightarrow B$ transition. Moreover, in our calculations we do not have the real positronium channel and it is known that this channel can affect electronic excitation cross sections. The present agreement between our results and the experimental data is a nice surprise, but may be due to cancellation of the effects that are not considered in our calculations.

ACKNOWLEDGMENTS

F.A. thanks FAPESP (Fundação para o Amparo à Pesquisa do Estado de São Paulo) for financial support. M.A.P.L. was supported by a grant from CNPq (Conselho Nacional de Desenvolvimento Científico e Tecnológico).

[1] I. Makkonen, M. Hakala, and M. J. Puska, Phys. Rev. B **73**, 035103 (2006).
[2] N. Guessoum, P. Jean, and W. Gillard, Astron. Astrophys. **436**, 171 (2005).
[3] C. M. Surko, G. F. Gribakin, and S. J. Buckman, J. Phys. B **38**, R57 (2005).
[4] T. J. Murphy and C. M. Surko, Phys. Rev. A **46**, 5696 (1992).
[5] O. Sueoka, J. Phys. Soc. Jpn. **51**, 3757 (1982).
[6] P. G. Coleman, J. T. Hutton, D. R. Cook, and C. A. Chandler, Can. J. Phys. **60**, 584 (1982).
[7] S. Mori and O. Sueoka, J. Phys. B **27**, 4349 (1994).
[8] O. Sueoka, B. Jin, and A. Hamada, Appl. Surf. Sci. **85**, 59 (1995).
[9] P. Chaudhuri and S. K. Adhikari, Phys. Rev. A **57**, 984 (1998); Nucl. Phys. A **631**, 715C (1998); J. Phys. B **31**, 3057 (1999); **32**, 129 (1999).
[10] L. A. Parcell, R. P. McEachran, and A. D. Stauffer, Nucl. Instrum. Methods Phys. Res. B **143**, 37 (1998).
[11] L. A. Parcell, R. P. McEachran, and A. D. Stauffer, Nucl. Instrum. Methods Phys. Res. B **171**, 113 (2000).
[12] J. P. Sullivan, J. P. Marler, S. J. Gilbert, S. J. Buckman, and C. M. Surko, Phys. Rev. Lett. **87**, 073201 (2001).
[13] T. Mukherjee, S. Sur, and A. S. Ghosh, J. Phys. B **24**, 1449 (1991).
[14] M. Mukherjee, T. Mukherjee, and A. S. Ghosh, J. Phys. B **24**, L463 (1991).
[15] A. S. Ghosh and T. Mukherjee, Hyperfine Interact. **89**, 299 (1994).
[16] J. L. S. Lino, J. S. E. Germano, and M. A. P. Lima, J. Phys. B **27**, 1881 (1994).
[17] P. Chaudhuri, M. T. D. Varella, C. R. C. de Carvalho, and M. A. P. Lima, Nucl. Instrum. Methods Phys. Res. B **221**, 69 (2004).
[18] P. Chaudhuri, M. T. D. Varella, C. R. C. de Carvalho, and M. A. P. Lima, Phys. Rev. A **69**, 042703 (2004).
[19] J. P. Marler and C. M. Surko, Phys. Rev. A **72**, 062713 (2005).
[20] E. P. da Silva, M. T. D. Varella, and M. A. P. Lima, Phys. Rev. A **72**, 062715 (2005).
[21] K. Takatsuka and V. McKoy, Phys. Rev. A **24**, 2473 (1981).
[22] K. Takatsuka and V. McKoy, Phys. Rev. A **30**, 1734 (1984).

[23] J. S. E. Germano and M. A. P. Lima, Phys. Rev. A **47**, 3976 (1993).
[24] A. M. Machado, A. M. A. Taveira, L. M. Brescansin, and M.-T. Lee, THEOCHEM **574**, 133 (2001).
[25] T. H. Dunning, J. Chem. Phys. **53**, 2823 (1970).
[26] S. Huzinaga and M. Kolbukowski, Chem. Phys. Lett. **212**, 260 (1993).
[27] P. Carsky, V. Hrouda, and J. Michl, Int. J. Quantum Chem. **53**, 419 (1995); **53**, 431 (1995); P. Carsky, V. Hrouda, J. Michl, and D. Antic, *ibid.* **53**, 437 (1995).
[28] P. A. Fraser, Adv. At. Mol. Phys. **4**, 63 (1968).
[29] T. L. Gibson, M. A. P. Lima, V. McKoy, and W. M. Huo, Phys. Rev. A **35**, 2473 (1987).
[30] T. L. Gibson, M. A. P. Lima, K. Takatsuka, and V. McKoy, Phys. Rev. A **30**, 3005 (1984).
[31] M. A. P. Lima, T. L. Gibson, K. Takatsuka, and V. McKoy, Phys. Rev. A **30**, 1741 (1984).
[32] R. F. da Costa, F. J. da Paixão, and M. A. P. Lima, J. Phys. B **37**, L129 (2004).
[33] R. F. da Costa, F. J. da Paixão, and M. A. P. Lima, J. Phys. B **38**, 4363 (2005).
[34] W. J. Hunt and W. A. Goddard III, Chem. Phys. Lett. **3**, 414 (1969).
[35] S. E. Branchett and J. Tennyson, Phys. Rev. Lett. **64**, 2889 (1990).
[36] W. Kolos and J. Rychlewski, J. Mol. Spectrosc. **66**, 428 (1977).
[37] S. Rothenberg and E. R. Davidson, J. Chem. Phys. **44**, 730 (1966).
[38] T. E. Sharp, At. Data **2**, 119 (1971).
[39] T. L. Gibson, M. A. P. Lima, K. Takatsuka, and V. McKoy, Phys. Rev. A **30**, 3005 (1984); M. A. P. Lima, T. L. Gibson, K. Takatsuka, and V. McKoy, Phys. Rev. A **30**, 1741 (1984);
[40] M. A. P. Lima, L. M. Brescansin, A. J. R. da Silva, C. Winstead, and V. McKoy, Phys. Rev. A **41**, 327 (1990).
[41] T. N. Rescigno (private communication).
[42] J. L. S. Lino, J. S. E. Germano, E. P. da Silva, and M. A. P. Lima, Phys. Rev. A **58**, 3502 (1998).